International Journal of Material Forming (2023) 16:19
https://doi.org/10.1007/s12289-023-01741-8

DEVELOPMENTS IN MODELLING AND SIMULATION..JAPAN, SOUTH KOREA AND CHINA

A simple physics-based constitutive model to describe strain hardening in a wide strain range

Yongju Kim[1] · Gang Hee Gu[1] · Olivier Bouaziz[2,3] · Yuri Estrin[4,5] · Hyoung Seop Kim[1,6,7,8]

Received: 8 August 2022 / Accepted: 19 January 2023 / Published online: 28 January 2023

Abstract
It is almost commonplace to say that physics-based constitutive models developed to characterize the mechanical behavior of materials are to be preferred over phenomenological models. However, the constitutive relations offered by physics-based approaches are oftentimes too involved to be handled in finite element (FE) simulations for practical applications. There is a demand for physics-based, yet robust and user-friendly models, and one such model will be highlighted in this article. A simple constitutive model developed recently by Bouaziz to extend the classical physics-based Kocks-Mecking model provides a viable tool for modelling a broad range of materials – beyond the single-phase coarse-grained materials it was initially devised for. The efficacy of the model was put to the test by investigating its applicability for different materials. A broad interval of the true stress vs. true strain curve was studied by the measurement-in-neck-section method in the uniaxial tensile mode for six types of metallic materials, and simulations using the finite element method emulating the experimental conditions were developed. In this way, the engineering stress-strain curves were obtained corresponding to the true stress-strain curves for these materials. A comparison of the numerical simulations of the tensile behaviour of all six materials with the experimental results for a broad range of strains showed that among the models trialled, the Bouaziz model was the best-performing one. The proposed model can be recommended for use in FE simulations of the mechanical behaviour of engineering structures as a viable alternative to complex physics-based or simplistic phenomenological constitutive models.

Keywords Constitutive model · Strain hardening · Uniaxial tensile test · FEM simulation

Introduction

Measurements of the tensile true stress vs. true strain curves are the most common way to study the mechanical properties during plastic deformation [1–3]. However, in a uniaxial tensile test, the true stress-strain curve can be calculated from an engineering stress-strain curve only within the uniform deformation region [4], hence only a limited range of strain can be represented. To overcome this limitation, many experimental studies were conducted to characterize a wider range of true stress-strain curves using a digital image correlation (DIC) technique. The DIC technique can capture

✉ Hyoung Seop Kim
hskim@postech.ac.kr

1 Department of Materials Science and Engineering, Pohang University of Science and Technology (POSTECH), 37673 Pohang, Republic of Korea

2 Laboratoire d'Etude des Microstructures et de Mécanique des Matériaux (LEM3), CNRS, Université de Lorraine, Arts et Métier Paris Tech, 57000 Metz, France

3 LABoratoire d'EXcellence DAMAS, Université de Lorraine, 57000 Metz, France

4 Department of Materials Science and Engineering, Monash University, 3800 Clayton, VIC, Australia

5 Department of Mechanical Engineering, The University of Western Australia, 6009 Crawley, WA, Australia

6 Graduate Institute of Ferrous and Energy materials Technology (GIFT), Pohang University of Science and Technology (POSTECH), 37673 Pohang, Republic of Korea

7 Center for Heterogenic Metal Additive Manufacturing, Pohang University of Science and Technology (POSTECH), 37673 Pohang, Republic of Korea

8 Advanced Institute for Materials Research (WPI-AIMR), Tohoku University, 980-8577 Sendai, Japan

surface strains with high accuracy beyond the necking point where strain localization sets in [4–8]. In the present study, several constitutive models representing the observed strain hardening behavior were tested against this experimental evidence. The Bouaziz model was shown to provide the best description of the overall strain hardening behavior over the entire strain range, even beyond the necking point. At least for plastically isotropic materials, a generalization to the mechanical behavior in different (multiaxial) deformation modes is possible on the basis of the von Mises equivalent quantities, as reported in references [9–11].

In the industrial practice, the true stress-strain curves are commonly expressed in terms of constitutive models that require as few modeling parameters as possible. For example, the flow stress in the Hollomon model, the Swift model, and the Voce model can be defined as follows:

$$\sigma_{Hollomon} = \sigma_0 + K_H \varepsilon^{\mathrm{n}}, \tag{1}$$

$$\sigma_{Swift} = K_S\left(\varepsilon_0 + \varepsilon\right)^{\mathrm{n}}, \tag{2}$$

$$\sigma_{Voce} = \sigma_0 + \mathrm{A}(1 - \exp^{-\mathrm{B}\varepsilon}), \tag{3}$$

where $\mathrm{K_H}, \mathrm{K_S}$, n, A, and B are modeling parameters required to represent strain hardening behavior in terms of the axial strain (ε) and the frictional stress$\left(\sigma_0\right)$. However, these simple constitutive models cannot fully represent the initial yield strength and strain hardening of the experimentally obtained material's properties because their physical meaning is not considered [12–14]. Therefore, several physics-based constitutive models have been developed to describe strain hardening behavior based on the deformation mechanisms including dislocation glide and twinning [15, 16]. Although these physics-based models represent the evolution of dislocations and twins at micro-scale and ensure high accuracy in predicting the mechanical properties, they are somewhat difficult to use in practice as they involve many model parameters. In this study, a simple physics-based constitutive model is proposed and validated by comparing it with experimental data. The results demonstrate that the proposed model can be a viable alternative to complex dislocation-based constitutive models representing the mechanical properties of metallic materials.

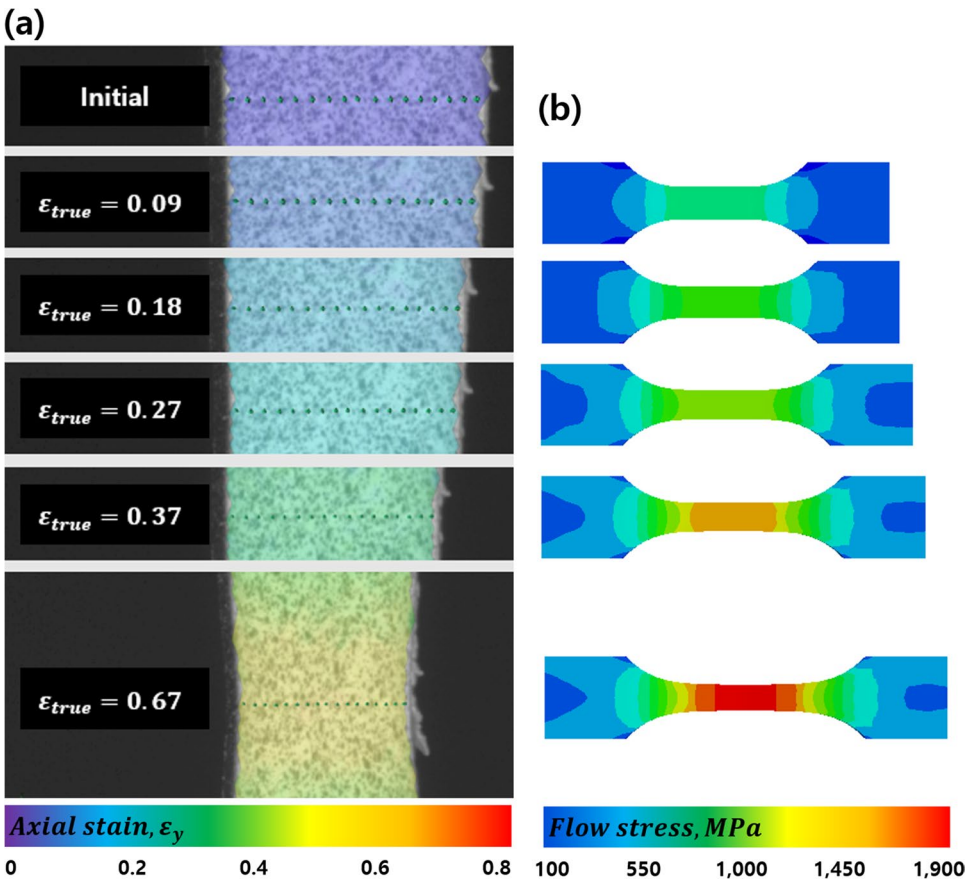

Fig. 1 **a** Distribution of the axial strain (ε_y) in TWIP steel with 17 equally spaced points selected in the neck region at various stages of the tensile test. **b** True stress distribution corresponding to the axial strain state (left) obtained by the FEM simulation

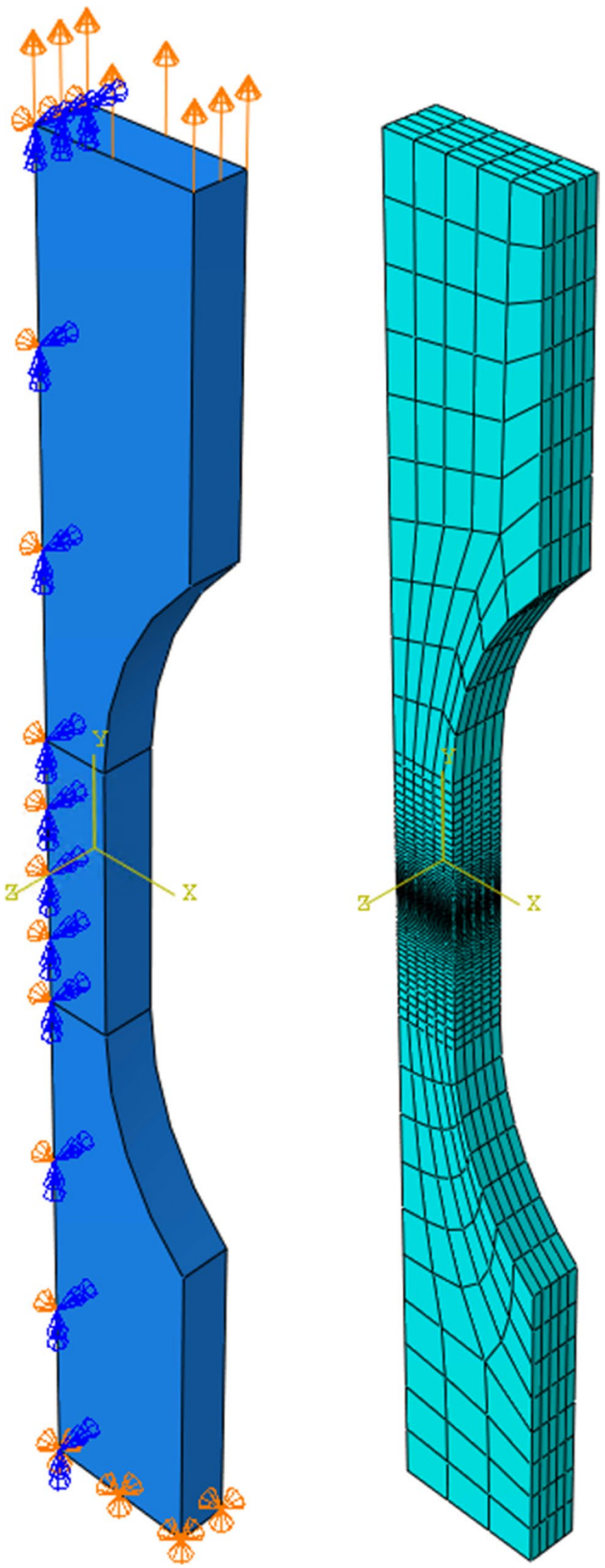

Fig. 2 Tensile specimen with applied mesh and boundary conditions in the FEM simulations

Table 1 Modeling parameters representing the long-range true stress-strain curves using the proposed models due to Hollomon, Swift, Voce, and Bouaziz as shown in Fig. 3

Materials	Thickness	E (GPa)	Hollomon model			Swift model			Voce model			Bouaziz model		
	(mm)		σ_0 (MPa)	K_H	n	K_S	ε_0	n	σ_0 (MPa)	A	B	σ_0 (MPa)	σ_s	θ_0
E-form Mg	0.90	29	155	268.84	0.41	394.33	0.00	0.18	155	144.25	15.44	155	50.22	3,709.49
Ti-6Al-4 V	1.01	104	1,056	1,326.42	0.68	1,458.52	0.01	0.07	1,056	286.99	10.51	1,056	118.34	4,228.49
AISI 316 L	0.98	113	284	2,217.77	0.83	1,521.57	0.03	0.50	284	1,196.09	2.31	284	714.10	3,083.36
DP980	1.19	178	814	710.23	0.37	1,430.47	0.01	0.10	814	518.25	8.97	814	142.73	1,1408.26
TRIP steel	0.98	146	1,095	544.72	0.49	1,904.20	0.01	0.13	1,095	645.20	6.58	1,095	259.34	5,914.46
TWIP steel	0.98	211	516	936.71	0.48	2,456.88	0.08	0.63	516	2,406.60	1.40	516	1,862.78	3,441.56

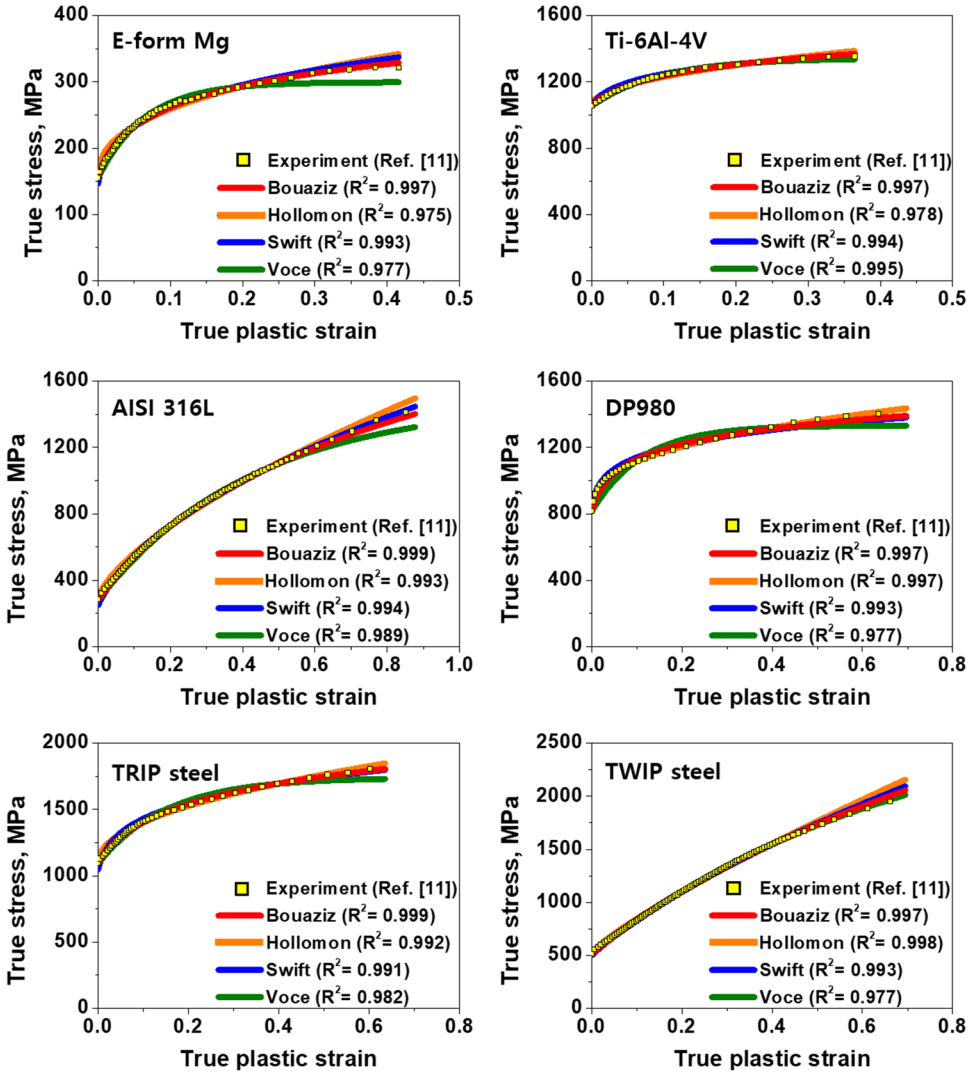

Fig. 3 Comparison of the true stress vs. true strain curves calculated by using the four constitutive models with the experimental data

Experiments and modeling

Phenomenological constitutive models expressed by the Hollomon Eq. (1), the Swift Eq. (2), and the Voce Eq. (3), have been broadly used for describing uniaxial stress-strain behavior and FEM simulations of deformation under multi-axial loading. The reason for their wide usage is the simplicity of the respective constitutive relations with just a few fitting parameters. However, a weak point of these models – with the exception of the Voce model, see below - is the lack of their physical interpretation. By contrast, microstructure-related models such as the Kocks-Mecking-Estrin (KME) model [17] or its progenitor, the Kocks-Mecking model [18] are based on sound physical considerations and incorporate microstructural features and the mechanisms underlying plastic deformation. However, this kind of models is hard to be implemented in FEM. Hence, a simpler constitutive model with fewer parameters is needed.

Recently, such a simple constitutive model was proposed by Bouaziz in Refs. [19, 20]. In this model, the flow stress is given by

$$\sigma_{Bouaziz} = \sigma_0 + \sigma_s \ln\left(1 + \frac{\theta_0}{\sigma_S}\varepsilon\right), \tag{4}$$

where σ_0 is the crystalline lattice 'friction' that can be interpreted as the yield strength associated with the initial resistance to dislocation glide based on the corresponding frictional shear stress; the θ_0 and σ_s are model parameters representing the competition between storage and annihilation of dislocations, respectively, as an extension of the Kocks-Mecking approach. The heuristic constitutive relation given by Eq. (4) recovers the classical physically based strain hardening law (the Kocks-Mecking law) for low strains and also accounts for large strain behavior considering the combination of the σ_s and θ_0 parameters.

These parameters have a clear physical interpretation, σ_s representing the asymptotically approached saturation stress

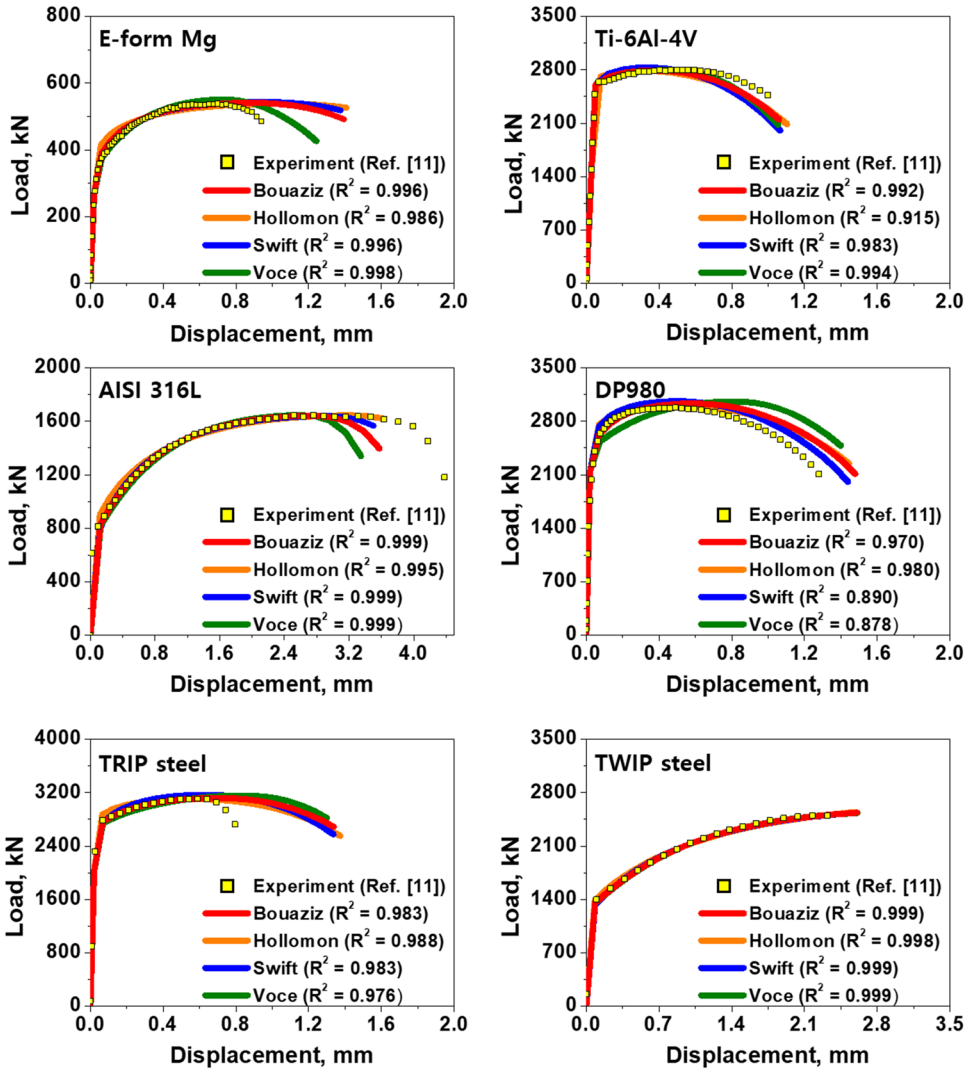

Fig. 4 Comparison of the load-displacement curves obtained by the FEM simulations with the experimental results

and θ_0 denoting the stage II strain hardening coefficient [18]. As a side remark, we should mention that the Voce equation follows from the Kocks-Mecking model, so that the parameters A and B in Eq. (2) can be directly related to σ_s and θ_0.

In order to assess the validity of the above constitutive models, a wide range of experimental stress-strain curves of various materials were employed. The dog bone-shaped specimens with different thicknesses depending on the type of metal were prepared with a width of 2.5 mm and a gauge length of 6.4 mm. The surface of the specimen was mechanically polished with 600, 800, and 1,200 silicon carbide grit, and then a commercial black and white spray was uniformly sprayed to measure the deformation of the specimen using the DIC technique. Thereafter, a uniaxial tensile test was performed at room temperature at a strain rate of 10^{-3} s^{-1} using a universal testing machine (Instron 1361, Instron Corp, USA). The measurement-in-neck-section method was employed as a type of DIC method (using ARAMIS 5 M, GOM, Germany) proposed in Ref. [5]. The true strain was estimated as the average strain at 17 equally spaced points in the transverse direction of the neck region (Fig. 1a) as follows:

$$\varepsilon_{true} = \frac{\sum_{i=1}^{i=n} \varepsilon_{y(i)}}{n}, \tag{5}$$

where $\varepsilon_{y(i)}$ is a local strain at the i-th point along the uniaxial direction. At this moment, the true stress was synchronized by finding the load in the corresponding strain state. Because the axial stress component exceeds by far the other stress components, it can be assumed that the load is mostly governed by the axial component. Since non-standard tensile specimens had to be employed in our experiments, we had to resort to the averaging procedure for tensile strain. However, this procedure was shown not to compromise the tensile data obtained on the basis of the DIC technique. The DIC method employed was validated by previous studies [5, 6, 11, 21].

In addition, simulations of a uniaxial tensile test by FEM were used to validate engineering stress-strain curves. This was done for each constitutive model and each material tested by implementing a user-defined subroutine (UHARD) in commercial ABAQUS 6.17 software. The FEM model was designed to replicate the experimental conditions, such as the specimen geometry and the loading conditions, as shown in Fig. 2. The adequate number of elements was determined by comparing them with the experimental results. All six types of metallic materials investigated were assumed to have the same Poisson's ratio of 0.3, and their elastic modulus and the appropriate values of the fitting parameters of the proposed Bouaziz model, along with those for the Hollomon, Swift, and Voce models, as summarized in Table 1. The latter was determined using the generalized reduced gradient (GRG) algorithm, set in the direction minimizing the difference between the experimental and numerical true stress-strain curves. The true stress distribution in the neck region is visualized in Fig. 1b, which was obtained by FEM simulations for the corresponding axial strain conditions (Fig. 1a).

Results and discussion

The true stress vs. true strain curves for the six materials studied (four steels, the Ti alloy, and the Mg alloy) calculated with the aid of the four models considered are shown in Fig. 3. They were fitted to the experimental data reported in [11]. The initial part of the true stress-strain curve obtained from the four constitutive models was in reasonably good agreement with most of the experimental results. The Bouaziz model was found to outperform the other three models, especially for the large-strain parts of the curves. This is reflected in the R^2 values for the fits being the highest for the Bouaziz model in most of the cases considered. This suggests that the evolution of the dislocation density expressed by this model is captured adequately by this model. A further forte of the model is that it contains just two adjustable parameters whose physical interpretation is straightforward.

In addition, uniaxial tensile tests were simulated by FEM using the four constitutive models. To obtain the load-displacement curves corresponding to each constitutive model, the elongated gauge length of the specimen was used to estimate the displacement, and the corresponding load values were obtained by applying a different thickness of the uniaxial tensile specimen (Table 1) for each material, as shown in Fig. 2. The results presented in Fig. 4 demonstrate that for materials exhibiting higher strain hardening, especially AISI 316 L and TWIP steel, the simulations agree well with the experimental data. Again, the Bouaziz model is seen to outperform the other three models considered. In particular, it represents the deformation behavior of DP980 at small strains better than the Swift and Voce models. We also note that the Voce model (and also the Kocks-Mecking one) follow from the Bouaziz model directly in the low strain part of the curve. These two models run into problems at large strains, whereas the Bouaziz model also accounts for the large strain part of the curve as well.

Conclusion

In this work, the models by Hollomon, Swift, Voce, and Bouaziz were compared with regard to their descriptive capability. These models are in the same 'league', as all of them involve just two adjustable parameters. In this 'contest of models', the strain hardening behavior they predict was compared with the experimental data for six metallic materials under uniaxial tensile deformation. The Bouaziz model was found to be in better general agreement with the strain hardening data. The 'runner-up', the Voce model, was almost on par with it in the description of the overall strain hardening behavior, but was outperformed by the Bouaziz model in the large-strain part of the deformation curves. The Bouaziz model can thus be seen as an apt extension of the classical Kocks-Mecking model for the strain range beyond the stage III hardening for which the latter has been developed. The fact that the model works so well for materials of different kinds and with a great diversity in chemical and phase composition demonstrates its surprising universality. With just two adjustable parameters, the model is very robust and user-friendly. Thus, this simple constitutive model should be applicable in simulating the mechanical behavior of a broad range of materials.

Acknowledgements This work was supported by the National Research Foundation of Korea (NRF) grant funded by the Korean government (MSIP) (NRF-2021R1A2C3006662) and (NRF-2022R1A5A1030054).

Declarations

Conflict of interest None.

References

1. Zhang ZL, Hauge M, Ødegård J, Thaulow C (1999) Determining material true stress-strain curve from tensile specimens with rectangular cross-section. Int J Solids Struct 36:3497–3516. https://doi.org/10.1016/S0020-7683(98)00153-X
2. Byun TS, Hashimoto N (2006) Strain hardening and long-range internal stress in the localized deformation of irradiated polycrystalline metals. J Nucl Mater 354:123–130. https://doi.org/10.1016/j.jnucmat.2006.02.099
3. Örnek C, Şeşen BM, Ürgen MK (2022) Understanding hydrogen-induced strain localization in super duplex stainless steel using

digital image correlation technique. Met Mater Int 28:475–486. https://doi.org/10.1007/s12540-021-01123-2
4. Zhu F, Bai P, Zhang J et al (2015) Measurement of true stress-strain curves and evolution of plastic zone of low carbon steel under uniaxial tension using digital image correlation. Opt Lasers Eng 65:81–88. https://doi.org/10.1016/j.optlaseng.2014.06.013
5. Gu GH, Moon J, Park HK et al (2021) Obtaining a wide-strain-range true stress–strain curve ysing the measurement-in-neck-section method. Exp Mech 61:1343–1348. https://doi.org/10.1007/s11340-021-00747-0
6. Gu GH, Ahn SY, Kim Y et al (2022) Determining reliable wide-strain-range equivalent stress–strain curves using 3D digital image correlation. J Mater Res Technol 19:2822–2830. https://doi.org/10.1016/j.jmrt.2022.06.054
7. Gu GH, Kim Y, Kim RE et al (2022) A new digital image correlation method for measuring wide strain range true stress–strain curve of clad materials. Met Mater Int 2–7. https://doi.org/10.1007/s12540-022-01219-3
8. Kim K, Il, Oh Y, Kim DU et al (2022) Strain analysis of multi-phase steel using in-situ EBSD tensile testing and digital image correlation. Met Mater Int 28:1094–1104. https://doi.org/10.1007/s12540-021-01044-0
9. Estrin Y (1996) Dislocation-density-related constitutive modelling. In: Krausz AS, Krausz K (eds) Unified Constitutive Laws of Plastic Deformation. Academic, pp 69–106. https://doi.org/10.1016/B978-012425970-6/50003-5
10. Pham QT, Lee BH, Park KC, Kim YS (2018) Influence of the post-necking prediction of hardening law on the theoretical forming limit curve of aluminium sheets. Int J Mech Sci 140:521–536. https://doi.org/10.1016/j.ijmecsci.2018.02.040
11. Kim Y, Gu GH, Asghari-Rad P et al (2022) Novel deep learning approach for practical applications of indentation. Mater Today Adv 13:100207. https://doi.org/10.1016/j.mtadv.2022.100207
12. Yang H, Li H, Ma J et al (2019) Constitutive modeling related uncertainties: effects on deformation prediction accuracy of sheet metallic materials. Int J Mech Sci 157–158:574–598. https://doi.org/10.1016/j.ijmecsci.2019.05.004
13. Sung JH, Kim JH, Wagoner RH (2010) A plastic constitutive equation incorporating strain, strain-rate, and temperature. Int J Plast 26:1746–1771. https://doi.org/10.1016/j.ijplas.2010.02.005
14. Gavrus A (2012) Constitutive equation for description of metallic materials behavior during static and dynamic loadings taking into account important gradients of plastic deformation. Key Eng Mater 504–506:697–702. https://doi.org/10.4028/www.scientific.net/KEM.504-506.697
15. Kim Y, Asghari-Rad P, Lee J et al (2022) Solid solution induced back-stress in multi-principal element alloys: experiment and modeling. Mater Sci Eng A 835:142621. https://doi.org/10.1016/j.msea.2022.142621
16. Kim Y, Jung J, Park HK, Kim HS (2022) Importance of microstructural features in bimodal structure–property linkage. Met Mater Int 4:1–6. https://doi.org/10.1007/s12540-022-01200-0
17. Bouaziz O, Barbier D, Embury JD, Badinier G (2013) An extension of the Kocks-Mecking model of work hardening to include kinematic hardening and its application to solutes in ferrite. Philos Mag 93:247–255. https://doi.org/10.1080/14786435.2012.704419
18. Kocks UF, Mecking H (2003) Physics and phenomenology of strain hardening: the FCC case. Prog Mater Sci 48:171–273. https://doi.org/10.1016/S0079-6425(02)00003-8
19. Bouaziz O, Lloyd D (2022) Assessment of a physical based modelling suitable to capture the mechanical behaviour at large plastic strain of aluminium alloys. Metall Res Technol 419:4–7. https://doi.org/10.1051/metal/2022064
20. Bouaziz O (2012) Revisited storage and dynamic recovery of dislocation density evolution law: toward a generalized kocks-mecking model of strain-hardening. Adv Eng Mater 14:759–761. https://doi.org/10.1002/adem.201200083
21. Gu GH, Kim RE, Ahn SE et al (2022) Multi-scale investigation on local strain and damage evolution of Al1050 / steel / Al1050 clad sheet. J Mater Res Technol 20:128–138. https://doi.org/10.1016/j.jmrt.2022.07.056